Density functional theory calculation for carrier scattering at 4H-SiC(0001)/SiO_2 interface

Kazuma Yokota
Graduate School of Engineering
Kobe University
Kobe, Japan
219t262t@stu.kobe-u.ac.jp

Nahoto Funaki
Graduate School of Engineering
Kobe University
Kobe, Japan
231t252t@stu.kobe-u.ac.jp

Mizuho Ohmoto
Graduate School of Engineering
Kobe University
Kobe, Japan
227t212t@stu.kobe-u.ac.jp

Mitsuharu Uemoto
Graduate School of Engineering
Kobe University
Kobe, Japan
https://orcid.org/0000-0002-2248-5665

Tomoya Ono
Graduate School of Engineering
Kobe University
Kobe, Japan
https://orcid.org/0000-0002-5607-6472

***Abstract*—Electronic structure and charrier scattering property of the 4H-SiC(0001)/SiO_2 interface are investigated by the density functional theory calculations. It is found that the bonding structure with SiO_2 affects the electronic structure of the interface. In addition, there are two conduction channels at the interface. The carriers flowing the channel immediately below the interface are significantly scattered at the step edge and those flowing the channel 5 Å away from the interface are insensitive to the existence of the step edges. These results indicate that on-current will increase when the on-axis SiC substrates are used for metal-oxide-semiconductor field-effect transistors because the density of the step edges is low at the on-axis substrates.**

***Index Terms*—Density functional theory, interface step, electronic structure, carrier scattering property**

I. Introduction

4H-silicon carbide (4H-SiC) is an IV-IV type semiconductor with a wide band gap of 3.2 eV, and the 4H-SiC based metal-oxide-semiconductor field-effect transistor (MOSFET) is expected to be used in next generation switching devices operating at high power and high frequency applications [1]. However, the potential of 4H-SiC has not been fully utilized owing to the low on current of MOSFETs, which is caused by defects at the 4H-SiC/SiO_2 interface. 4H-SiC(0001) surface intrinsically possesses atomic-scale step-and-terrace structures, which are generated during the fabrication process of 4H-SiC substrates. The electronic structure of the 4H-SiC/SiO_2 interface is significantly affected by the interface atomic configuration [2] and the spatial deviations of the electronic structures scatter the carriers [3]. Therefore, the step-and-terrace structures are also expected to affect the on current. We investigate the electronic structure and carrier scattering property at the step edges by density functional theory (DFT) [4] calculation.

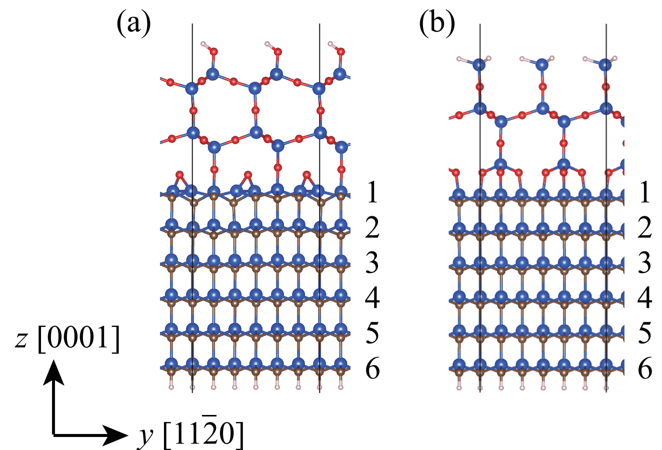

Fig. 1. Computational model for 4H-SiC(0001)/SiO_2 interface without steps. (a) One-bridging-bond and (b) three-bridging-bond structures. Blue, brown, red, and white spheres indicate Si, C, O, and H atoms, respectively. The numbers written on the right-hand-side of the atomic structures are the indices of the atomic layers.

II. Electronic structure of interface without steps

First, let us introduce the electronic structure of the 4H-SiC(0001)/SiO_2 interface without steps investigated in our previous study [2], [5]. We proposed the interface atomic structures of the SiO_2 on 4H-SiC(0001) substrate, in which the Si atoms of the SiO_2 region are connected to the Si atoms in the 4H-SiC(0001) substrate via one- or three-bridging-bond structure. The interface model, where the first interface SiC bilayer is at the k site and the atomic configuration of SiO_2 region is one-bridging-bond structure, is referred as the k1 interface model and the other interface models are similarly named the k3, h1, and h3 interface models. Figure 1 shows the computational models. We illustrate only the k1 and k3

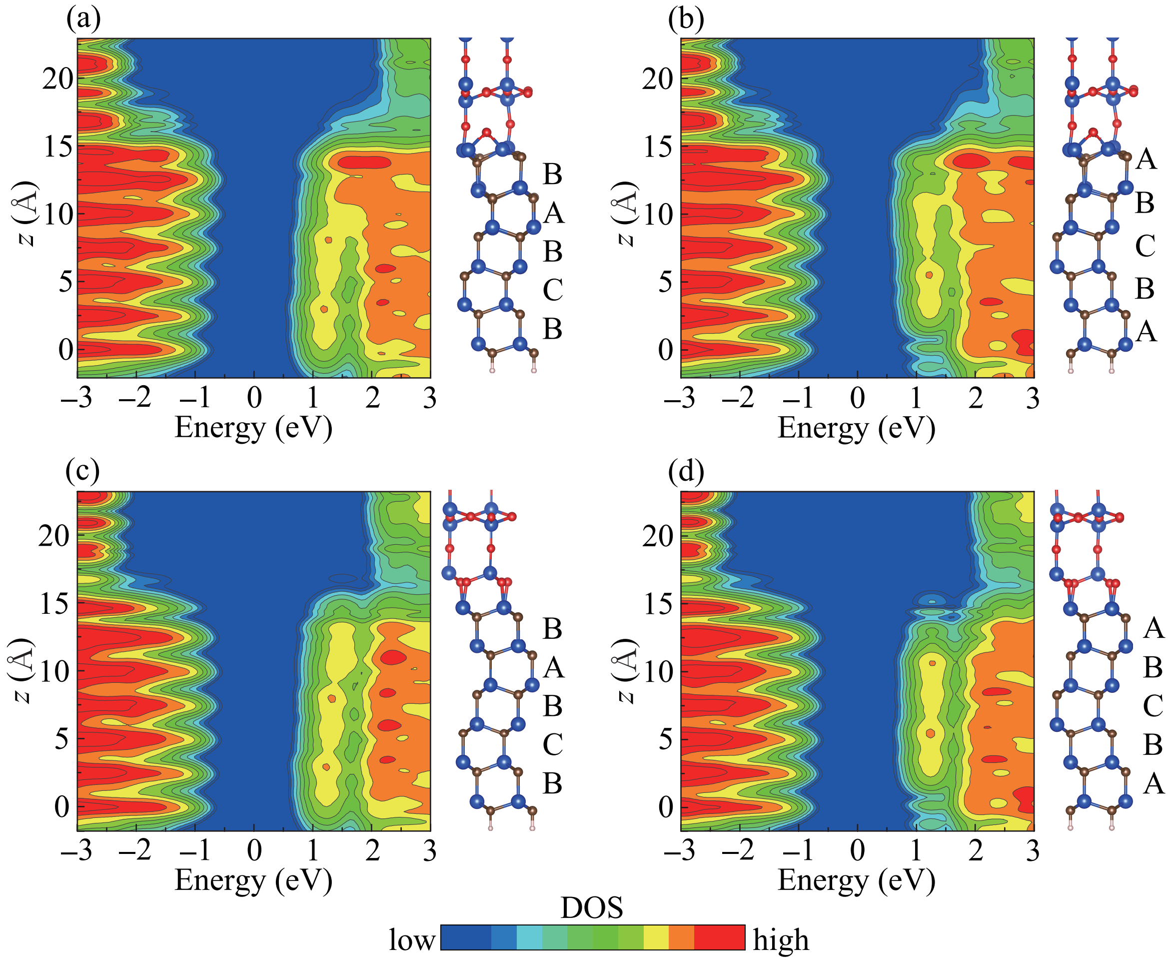

Fig. 2. LDOS of 4H-SiC(0001)/SiO_2 interface without steps for (a) h1, (b) k1, (c) h3, and (d) k3 interface models. Zero energy is chosen as the Fermi energy. Each contour represents twice or half the density of the adjacent contours and the lowest contour is 6.94×10^{-6} electron/eV/Å. The vertical axis is the height of the model. For clarity, structural models are provided to the right of each distribution. (Reprinted with permission from Ref. [5], copyright 2017 the American Physical Society.)

interface models because the atomic structures of the k and h sites appear the same when they are seen from the $[1\bar{1}00]$ direction. The z-axis was taken to be the direction perpendicular to the interface. We employed the rectangular supercells of $5.33 \times 9.24 \times 37.26$ Å^3. Integration over the Brillouin zone was carried out using a 2×2 k-point mesh. A vacuum gap of 12 Å thickness was inserted between the slabs under the periodic boundary condition. It is reported that most of SiO_2 in the SiC(0001)/SiO_2 interface is amorphous. However, we employed the crystaline atomic structure models proposed on the basis of scanning transmission electron microscopy images [5] because the modeling of the interface with SiC and amorphous SiO_2 is not easy in DFT calculations. We used the RSPACE code [6]–[8], which is based on the real-space finite-difference approach [9] within the frameworks of DFT. We employed the local density approximation [10] of the DFT to describe the exchange and correlation effects. Electron-ion interactions were approximated by the projector-augmented wave method [11]. The structural optimization was performed until the residual forces are smaller than 0.001 Hartree/Bohr radius.

The local density of states (LDOS) was calculated as

$$\rho(z, E) = \sum_{i,k} \int |\Psi_{i,k}(x, y, z)|^2 \mathrm{d}x\mathrm{d}y \times N\mathrm{e}^{-\alpha(E-\varepsilon_{i,k})^2},$$

where $\varepsilon_{i,k}$ are the eigenvalues of the wavefunction $\Psi_{i,k}$ with indexes i and k denoting the eigenstate and the k-point, respectively, z is the coordinate of the plane where the LDOS is plotted, and $N(= \sqrt{\frac{\alpha}{\pi}} \cdot \frac{1}{N_k})$ is the normalization factor with α as the smearing factor and N_k as the number of k-points in the Brillouin zone. Here, α is set to 8.2 eV^{-2}.

Figure 2 shows the LDOS of the interface without steps. Since n-channel MOSFETs are more widely used for SiC-MOSFET than p-channel MOSFETs, the behavior of the conduction band edge (CBE) states plays an important role. It was found that the CBE states appear at the second interface bilayer in the k1 and k3 interface models. On the other hand,

the CBE states appear at the first interface bilayer in the h3 interface model while they lie at the third bilayer in the h1 interface model [2], [5]. The exitance of the CBE states was explained by the electrostatic potential in the 4H-SiC(0001) substrate [12] and the CBE states always appear at the h site. Therefore, the CBE states lie at the second interface bilayer in the k1 and k3 interface models. In the h1 interface model, due to the strong electron negativity of the O atoms bridging Si atoms at the first bilayer, the CBE states disappear at the first and second interface bilayers and lie at the third bilayer.

III. Electronic structure of interface with atomic-scale steps

Now, we investigate the electronic structure of the interface with atomic-scale steps. Hereafter, we refer to the interface with atomic-scale steps as the step interface. Figure 3 shows the computational model, where the trench structure model is employed to imitate the step interface. In the case of 4H-SiC(0001) substrates, h and k sites of SiC bilayers stack alternatively. When the upper terrace is at h site, the lower terrace is always at k site. Moreover, when the SiO_2 region of the upper terrace is one-bridging-bond structure, that of the lower terrace is three-bridging-bond structure. For the step interface, the model, where the upper terrace is the h1 structure and the lower terrace is the k3 structure, is employed. The rectangular supercells of $5.33 \times 36.96 \times 40.44$ Å^3 is used. A vacuum gap of 14.1 Å thickness is inserted between the slabs under the periodic boundary condition. The other computational conditions are the same to those for the interface without steps.

We focus on the behavior of the CBE states of the step interface. Figure 4 shows the LDOS. As expected from the interface without steps, the CBE states lie at the third bilayer in the step interface.

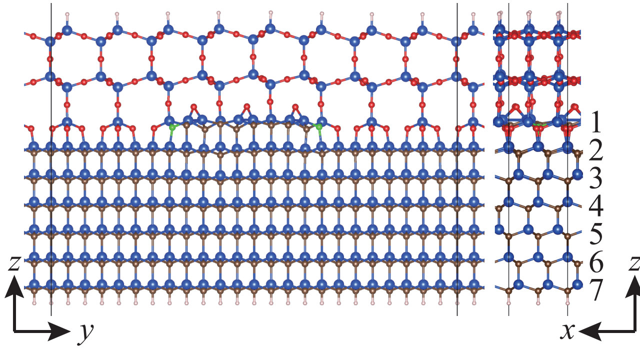

Fig. 3. Computational model for 4H-SiC(0001)/SiO_2 step interface. Blue, brown, red, white, and green spheres indicate Si, C, O, H, and N atoms, respectively. The numbers written on the right-hand-side of the atomic structure are the indices of the atomic layers counted from the upper terrace.

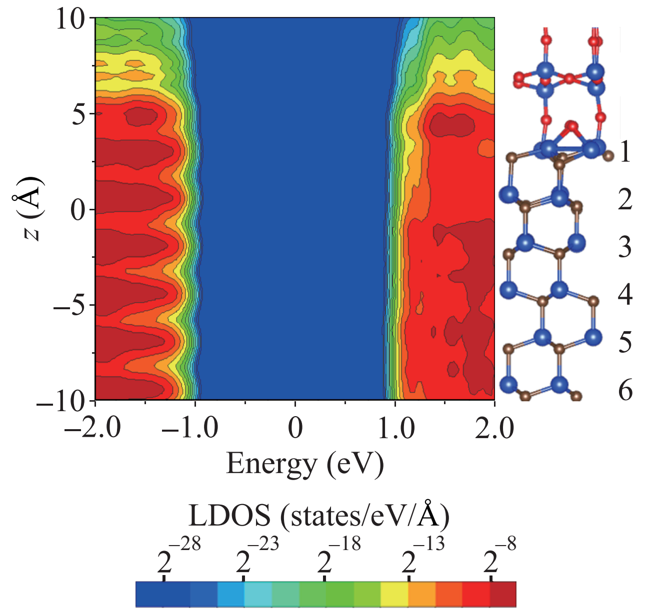

Fig. 4. LDOS of 4H-SiC(0001)/SiO_2 step interface. Atomic structure is illustrated as a visual aid and the numbers written on the right-hand-side of the atomic structure are the indices of the atomic layers counted from the upper terrace.

IV. Carrier transport property of interface with atomic-scale steps

Let us explore the carrier transport property of the step interface. Carrier transport calculation is performed by RSPACE code [7], [13]. Electron-ion interactions are approximated by the norm-conserving pseudopotentials [14] contained in NCPS2K database [15]. The other computational conditions are the same to those for the electronic-structure calculation. Figure 5 shows the transmission spectrum. There are two conduction channels. The transmission spectrum for the channel 1 is almost unity while that for the channel 2 is remarkably reduced. Figure 6 shows the charge density distribution of the scattering wave functions. It is found that the electrons in the channel 1 flow at the fifth bilayer while those in the channel 2 flow in the vicinity of the interface. In addition, the electrons in the channel 2 is refracted at the step edges. Therefore, it is fair to conclude that the carriers flowing near the interface are strongly affected by the interface atomic structure while those in the substrate are insensitive.

V. Conclusion

We have investigated the electronic structure and carrier transport property of the 4H-SiC(0001)/SiO_2 interface by the DFT calculation. It is found that the behavior of the CBE states is strongly affected by the atomic structure of the interface. In addition, carrier-scattering property calculations revealed that the carriers flowing at the bilayer 5 Å away from the interface are not scattered at the step edge while those flowing immediately below the interface are scattered at the step edges. Our results indicate that the carrier scattering will be reduced at on-axis surfaces because the density of step edge is low at the on-axis surfaces.

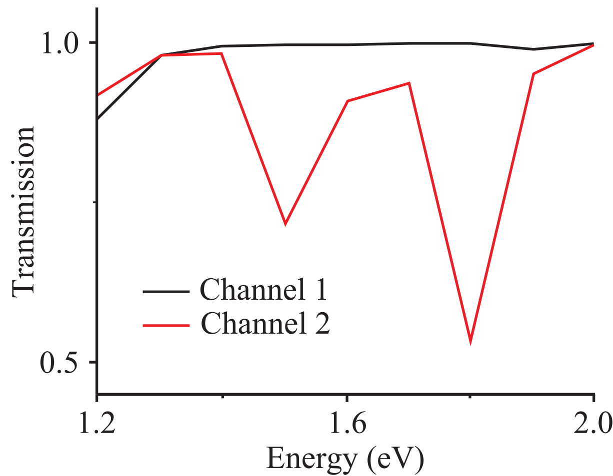

Fig. 5. Transmission spectrum. Zero of energy is chosen to the Fermi energy.

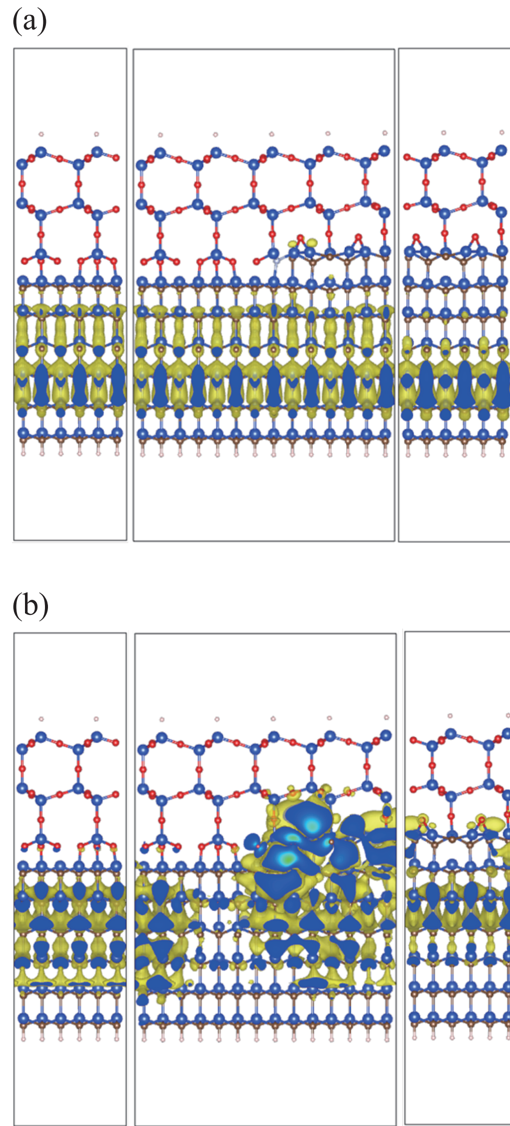

Fig. 6. Charge density distribution of scattering waves of (a) channel 1 and (b) channel 2. The left, center, and right panels indicate the left electrode, scattering, and right electrode regions, respectively. Carriers are injected from the left electode.

Acknowledgment

This work was partially financially supported by MEXT as part of the "Program for Promoting Researches on the Supercomputer Fugaku" (Quantum-Theory-Based Multiscale Simulations toward the Development of Next-Generation Energy-Saving Semiconductor Devices, JPMXP1020200205) and also supported as part of the JSPS KAKENHI (JP22H05463), JST CREST (JPMJCR22B4), and JSPS Core-to-Core Program (JPJSCCA20230005). The numerical calculations were carried out using the computer facilities of the Institute for Solid State Physics at The University of Tokyo, the Center for Computational Sciences at University of Tsukuba, and the supercomputer Fugaku provided by the RIKEN Center for Computational Science (Project ID: hp230175).

References

[1] T. Kimoto and H. Watanabe, "Defect engineering in SiC technology for high-voltage power devices," Appl. Phys. Express, vol. 13, pp. 120101 1-44, November 2020.

[2] C.J. Kirkham and T. Ono, "First-principles study on interlayer states at the 4H-SiC/SiO_2 interface and the effect of oxygen-related defects," J. Phys. Soc. Jpn. vol. 85, pp. 024701 1–5, February 2016.

[3] S. Iwase, C.J. Kirkham, and T. Ono, "Intrinsic origin of electron scattering at the 4H-SiC(0001)/SiO_2 interface," Pyhs. Rev. B, vol. 95, pp. 041302(R) 1–6, January 2017.

[4] P. Hohenberg and W. Kohn, "Inhomogeneous electron gas," Phys. Rev. vol. 136, pp. B864–B871, November 1964.

[5] T. Ono, C.J. Kirkham, S. Saito, and Y. Oshima, "Theoretical and experimental investigation of the atomic and electronic structures at the 4H-SiC(0001)/SiO_2 interface," Phys. Rev. B, vol. 96, pp. 115311 1–8, September 2017.

[6] T. Ono and K. Hirose, "Timesaving double-grid method for real-space electronic-structure calculations," Phys. Rev. Lett. vol. 82, pp. 5016–5019, June 1999.

[7] K. Hirose, T. Ono, Y. Fujimoto, and S. Tsukamoto, *First principles calculations in real-space formalism, electronic configurations and transport properties of nanostructures* (Imperial college, London, 2005).

[8] T. Ono, M. Heide, N. Atodiresei, P. Baumeister, S. Tsukamoto, and S. Blügel, "Real-space electronic structure calculations with full-potential all-electron precision for transition metals," Phys. Rev. B, vol. 82, pp. 205115 1–10, November 2010.

[9] J.R. Chelikowsky, N. Troullier, and Y. Saad, "Finite-difference-pseudopotential method: Electronic structure calculations without a basis," Phys. Rev. Lett., vol. 72, pp. 1240–1243, February 1994.

[10] S. H. Vosko, L. Wilk, and M. Nusair, "Accurate spin-dependent electron liquid correlation energies for local spin density calculations: a critical analysis," Can. J. Phys., vol. 58, pp. 1200–1211, August 1980.

[11] P. E. Blöchl, "Projector augmented-wave method," Phys. Rev. B, vol. 50, pp. 17953–17979, December 1994.

[12] Y.-i. Matsushita, S. Furuya, and A. Oshiyama, "Floating Electron States in Covalent Semiconductors," Phys. Rev. Lett., vol. 108, pp. 246404 1–5, June 2012.

[13] T. Ono, Y. Egami, K. Hirose, "First-principles transport calculation method based on real-space finite-difference nonequilibrium Green's function scheme," Phys. Rev. B, vol. 86, pp. 195406 1–13, November 2012.

[14] N. Troullier and J.L. Martins, "Efficient pseudopotentials for plane-wave calculations," Phys. Rev. B, vol. 43, pp. 1993–2006, September 1991.

[15] K. Kobayashi, "Norm-conserving pseudopotential database (NCPS97)," Comput. Mater. Sci., vol. 14, pp. 72–76, February 1999.